IJC Heart & Vasculature 55 (2024) 101510

Contents lists available at ScienceDirect

IJC Heart & Vasculature

journal homepage: www.sciencedirect.com/journal/ijc-heart-and-vasculature

Test-retest reproducibility of absolute myocardial blood flow obtained using stress dynamic CT myocardial perfusion imaging

Daisuke Hasegawa [a], Satoshi Nakamura [b,*], Masafumi Takafuji [a], Hajime Sakuma [a], Kakuya Kitagawa [b,c]

[a] Department of Radiology, Mie University Hospital, Tsu, Japan
[b] Department of Advanced Diagnostic Imaging, Mie University Graduate School of Medicine, Tsu, Japan
[c] Regional Co-creation Deployment Center, Mie Regional Plan Co-creation Organization, Tsu, Japan

ARTICLE INFO

Keywords:
Myocardial Blood Flow
Dynamic CT Myocardial Perfusion Imaging
Coronary Artery Disease
Coronary Microvascular Disease
Test-retest Reproducibility

ABSTRACT

Background: Coronary artery disease (CAD) and coronary microvascular disease (CMD) are significant contributors to angina pectoris, necessitating reliable diagnostic techniques for effective management. While positron emission tomography has been the non-invasive gold standard for myocardial blood flow (MBF) quantification, stress dynamic CT myocardial perfusion imaging (CTMPI) has emerged as a promising alternative. This study aimed to evaluate the test–retest reproducibility of MBF measurements obtained using dynamic CTMPI.

Methods: The study retrospectively analyzed MBF values from two dynamic CTMPI examinations conducted in the same patient cohort (n = 30) to examine the consistency of MBF quantification and the ability to visually detect and grade abnormal perfusion suggesting ischemia between the tests. Global and remote MBF were defined as the mean MBF and the maximum MBF of all segments, respectively.

Results: MBF quantification revealed strong linear correlations between the tests (r = 0.89 for global MBF, r = 0.88 for remote MBF, and r = 0.82 for all segments), and intraclass correlation coefficients reflected high agreement between the tests (0.94 for global MBF, 0.93 for remote MBF, and 0.90 for all segments). Bland-Altman plots indicated a negligible mean difference with acceptable limits of agreements between the tests for global MBF, remote MBF, and all segments. Visual assessment of the CTMPI maps for abnormal perfusion suggesting ischemia yielded a good inter-test agreement with a weighted kappa value of 0.80.

Conclusion: Dynamic CTMPI can consistently reproduce absolute MBF values and reliably detect myocardial perfusion abnormalities, potentially making it a robust diagnostic tool for evaluating the presence and severity of CAD and CMD.

1. Introduction

Angina pectoris is a syndrome characterized by chest pain resulting from myocardial ischemia [1]. It not only reduces the quality of life but also leads to serious events such as acute coronary syndromes and sudden death from fatal arrhythmias [2]. Historically, the atherosclerotic narrowing of epicardial coronary arteries has been considered as a primary cause of angina. However, many patients display angina-like symptoms without significant stenotic lesions on coronary angiography. Furthermore, some patients with coronary stenosis still experience chest pain even after coronary revascularization [3]. Thus, the etiology of angina pectoris is not limited to the narrowing of epicardial coronary arteries alone, indicating that ischemia might also arise from other mechanisms.

The coronary vasculature includes epicardial arteries, prearteriolar vessels, arterioles, and capillaries. Coronary microvascular disease (CMD) affects the smaller components of this system—the arterioles and capillaries—resulting in myocardial ischemia even without significant epicardial coronary artery disease [4]. The pathophysiology of CMD encompasses endothelial dysfunction, abnormal vasodilation, or

Abbreviations: CAD, coronary artery disease; CFR, coronary flow reserve; CT, computed tomography; CTMPI, computed tomography myocardial perfusion imaging; CMD, coronary microvascular disease; IMR, index of microcirculatory resistance; MBF, myocardial blood flow; MPI, myocardial perfusion imaging; PET, positron emission tomography.

* Corresponding author at: Department of Advanced Diagnostic Imaging, Mie University Graduate School of Medicine, 2-174 Edobashi, Tsu, Mie 514-8507, Japan.
E-mail address: s-nakamura@med.mie-u.ac.jp (S. Nakamura).

https://doi.org/10.1016/j.ijcha.2024.101510
Received 19 June 2024; Received in revised form 6 September 2024; Accepted 12 September 2024
Available online 16 September 2024

microvascular spasm, all of which impair blood flow and oxygen delivery to the myocardium [5]. It is reported that 17 % of patients with chest pain symptoms have CMD, with no significant stenosis in the epicardial vessels as detected by invasive coronary angiography [6]. Accurate CMD diagnosis might be helpful for making the appropriate choice of treatment and avoiding unnecessary percutaneous coronary interventions.

Despite carrying a greater volume of myocardial blood flow than the epicardial vessels, the coronary microvasculature is challenging to visualize directly. Instead, its function is inferred from measurements of microcirculatory resistance using invasive catheterization or from myocardial blood flow (MBF) as determined by non-invasive stress imaging [5]. Consequently, when assessing CMD non-invasively, quantifying MBF through stress imaging is critical to determine the presence or absence of CMD. Positron emission tomography (PET) is known as the non-invasive gold standard for MBF quantification, providing reproducible MBF and myocardial flow reserve measurements with high diagnostic value [7].

Recent advances have made cardiac CT an alternative modality for estimating MBF non-invasively. Stress dynamic CT myocardial perfusion imaging (CTMPI) allows for the detection of hemodynamic significant stenosis though the quantification of MBF [8]. Importantly, dynamic CTMPI, when combined with coronary CT angiography (CCTA), provides simultaneous information on coronary anatomy and myocardial perfusion, clarifying the hemodynamic status for CAD on CCTA [9,10]. In addition to assessing CAD, dynamic CTMPI might be helpful in patients without significant stenosis to detect the presence or absence of CMD which appears as reduced absolute MBF. However, consistent and reproducible measurements of MBF by dynamic CTMPI may be essential for detecting abnormal perfusion, whether due to CAD or CMD. Unless MBF assessed by dynamic CTMPI could be consistently measured as reproducible absolute values across multiple tests, it could not serve as a critical indicator for the evaluation of ischemia due to CAD as well as CMD. Nevertheless, the reproducibility of quantitative MBF values acquired through dynamic CTMPI is scarcely documented. This study aimed to evaluate the test–retest reproducibility of MBFs obtained from two dynamic CTMPI exams performed in the same patient.

2. Methods

2.1. Study design

The study included 120 patients aged 45–85 with suspected or known CAD who underwent two comprehensive cardiac CTs between August 2014 and July 2020 at Mie university hospital. Of those patients, we excluded 90 patients who had coronary interventions between the two cardiac tests (n = 46), persistent atrial fibrillation (n = 30), the use of adenosine triphosphate (ATP) dose other than 200 μg/kg/min in the cardiac CTs (n = 10), and non-diagnostic dynamic CTMPI images due to severe artifacts (n = 4). Therefore 30 patients comprised the final study population. The median interval between the two tests was 795 days (interquartile range, 543 to 1068 days). None of the patients experienced cardiovascular events or developed new chest pain during this period. The institutional review board in our hospital approved the protocols for this retrospective study and waived the need to obtain individual consent based on the retrospective design.

2.2. Image acquisition

Patients were required to be fasting for at least 4 h and abstain from caffeine at least 12 h before the CT examination. The patient lied supine in the scanner and attached to an electrocardiogram (ECG) monitor and automated blood pressure monitor. Two 20–22 gauge IV lines, one for contrast agent administration in the right antecubital vein and a second for ATP administration in the left antecubital vein were placed. After anteroposterior and lateral topograms, unenhanced CT images for coronary artery calcium scoring were performed using prospectively ECG triggered high-pitch spiral scan with tube voltage of 120 kV. Then, second unenhanced CT images for extracellular volume estimation for future analysis were acquired.

After the unenhanced CT scan, during the administration of 20 mg of ATP at 200 μg/kg/min for >3 min, scan acquisition of dynamic CTMPI was initiated by injecting 40 mL of iopamidol with an iodine concentration of 370 mg/mL at a flow rate of 5 mL/s, followed by a 40 mL saline flush. Dynamic datasets were acquired in the end-systolic phase (triggered at 250 msec after the R wave) for 30 s via ECG-triggered axial scan mode repeated at two alternating table positions (i.e. “shuttle mode”) to obtain a z-axis coverage of 73 mm or 105 mm for the second- or third-generation scanner, respectively. The acquisition parameters of dynamic CTMPI in the 2nd or 3rd-generation scanner were as follows: collimation = 32 × 1.2 or 48 × 1.2 mm, rotation time = 0.28 or 0.25 s, and tube voltage = 80 or 70 kV, respectively. Tube current was determined using an automatic exposure control system with a quality reference of 350 at 120 kV or 300 mAs/rotation at 80 kV. After completing data acquisition, ATP administration was stopped. ECG, blood pressure, and arterial oxygen saturation were monitored and recorded throughout the procedure.

Ten minutes after dynamic stress CTMPI, standard prospective CCTA was performed at rest by bolus injection of 26mgI/kg/sec of iopamidol over 12 s with the coronary arteries dilated with a nitrate. Heart rate was controlled before CCTA with intravenous injection of landiolol hydrochloride (Corebeta, Ono Pharmaceutical Co., Ltd, Osaka, Japan), if necessary. The acquisition parameters of CCTA in the 2nd or 3rd-generation scanner were as follows: collimation = 128 × 0.6 or 192 × 0.6 mm, rotation time = 0.28 or 0.25 s, and tube voltage = automated tube voltage selection by CARE kV (Siemens Healthineers, Germany), respectively. Tube current was determined using the automatic exposure control system with the quality reference of 350 or 300 mAs/rotation at 120 kV. Axial images of CCTA were reconstructed with the smooth kernel (I26 or Br40) and iterative reconstruction technique (strength 3, SAFIRE or ADMIRE, Siemens). Reconstructed thickness and increments were 0.6 mm and 0.3 mm, respectively.

2.3. Image analysis

The analysis of dynamic CTMPI images was performed using commercially available perfusion software (Syngo VPCT body, Siemens Healthcare). MBF was estimated using a dedicated parametric deconvolution technique, based on a 2-compartment model of the intravascular and extravascular spaces. The maximum slope of time attenuation curves fitted for every voxel was used to generate a MBF map of 3 mm thickness and 1 mm increments. Polygonal regions of interest that measured 1 to 2 cm^2 were placed within the endocardial and epicardial sides in the 16 myocardial segments (according to the American Heart Association), excluding an apical segment, in the short-axis view on the MBF map. Global MBF was defined as a mean value of MBFs in all segments. Remote MBF was defined as the maximum MBF among the endocardial and epicardial MBFs of the 16 myocardial segments. The presence and severity of abnormal perfusion that suggests myocardial ischemia on the MBF map were assessed visually for each of 16 myocardial segments by two radiologists with more than 10 years of experience in dynamic CTMPI in a joint reading based on a four-point scale (Fig. 1): Grade 0 = normal; Grade 1 = mildly abnormal, not suggestive of ischemia; Grade 2 = moderately abnormal, potentially suggestive of ischemia; and Grade 3 = severely abnormal, strongly suggestive of ischemia. When evaluating abnormal perfusion suggestive of ischemia within each myocardial segment, the observers focused on visually assessing the relative distribution of myocardial perfusion across the segments, rather than relying on the absolute MBF values of individual segments.

CCTA images were visually evaluated by two radiologists with more than 10 years of experience in CCTA in a joint reading. Coronary

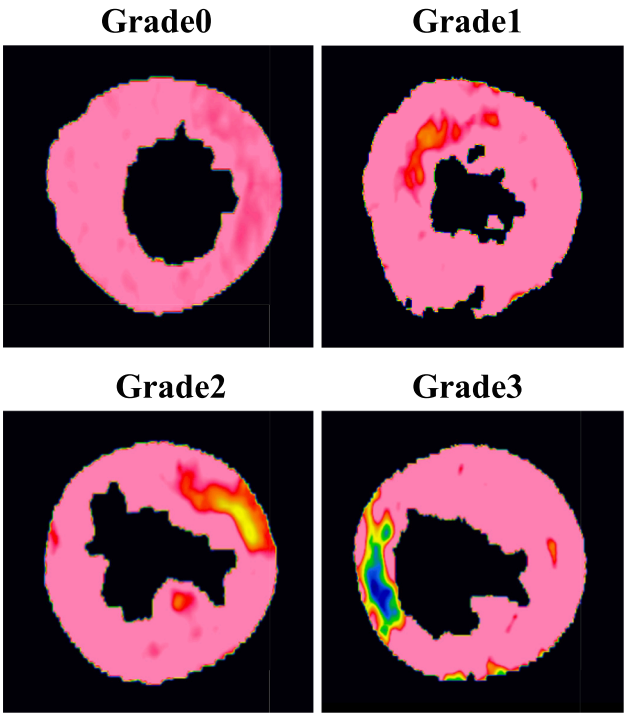

Fig. 1. Examples of a four-point scale for assessing abnormal perfusion that suggest myocardial ischemia on the MBF map. Grade 0 = normal; Grade 1 = mildly abnormal, not suggestive of ischemia; Grade 2 = moderately abnormal, potentially suggestive of ischemia; and Grade 3 = severely abnormal, strongly suggestive of ischemia. MBF=myocardial blood flow.

segments with a reference diameter ≥1.5 mm were assessed for the detection of stenosis. Severity of CAD on CTA was ranked by the Coronary Artery Disease-Reporting and Data System (CAD-RADS): 0 (0 %), 1 (1 % to 24 %), 2 (25 % to 49 %), 3 (50 % to 69 %), 4A (70 % to 99 % in 1 to 2 vessels), 4B (70 % to 99 % in 3 vessels or ≥50 % left main), or 5 (100 %).

2.4. Statistical analysis

Continuous variables are presented as mean ± SD, while categorical variables are expressed as frequency (percentage). The relationships between 1st and 2nd MBFs were assessed using Pearson correlation coefficient and linear regression analysis. The degree of agreement between 1st and 2nd MBFs was evaluated according to the Bland-Altman method and intraclass correlation coefficient (ICC). The agreement of the abnormal perfusion assessments between the two dynamic CTMPI exams was investigated using weighted kappa. All analyses were conducted using the R statistical software, version 3.4.4 (R Foundation for Statistical Computing).

3. Results

3.1. Patient characteristics

Table1 summarized characteristics of the 30 patients, with nearly half being male (47 %). The mean age was 70 ± 7 years and the body mass index 23 ± 3. Many of these patients have coronary risk factors, with 73 % having hypertension, 83 % dyslipidemia, 40 % diabetic, and 37 % a history of smoking. Additionally, 43 % of the patients have a history of myocardial infarction, and a high prevalence of prior coronary revascularization is observed at 87 %, mostly through percutaneous coronary intervention only (80 %). The mean time from the last revascularization to the first CTMPI was 5.9 ± 4.8 years. Symptoms included typical (23 %), atypical (10 %) chest pain and dyspnea (10 %).

Table 1
Patient characteristics.

Characteristic	All patients (n = 30)
Male	14 (47)
Age (mean ± SD)	70 ± 7
Body mass index (mean ± SD)	23 ± 3
Coronary risk factors	
Hypertension	22 (73)
Dyslipidemia	25 (83)
Diabetes	12 (40)
Smoking history	11 (37)
History of myocardial infarction	13 (43)
Prior coronary revascularization	26 (87)
PCI only	24 (80)
CABG only	1 (3)
Both	1 (3)
Time (year) from last revascularization to 1st CTMPI (mean ± SD)	5.9 ± 4.8
Symptom	
Typical chest pain	7 (23)
Atypical chest pain	3 (10)
Dyspnea	3 (10)
Echocardiography	
Left ventricular ejection fraction (mean ± SD)	68 ± 7
Left ventricular wall motion abnormality	9 (30)
Medication at 1st CTMPI	
Antiplatelet drugs	28 (93)
Anticoagulants	1 (3)
Calcium channel blockers	16 (53)
ACE/ARB	17 (57)
Nitrates	8 (27)
Beta blockers	9 (30)
Diuretics	2 (7)
Statins	25 (83)
Cholesterol Absorption Inhibitor	4 (13)
GLP-1 receptor agonists	1 (3)
DPP-4 inhibitors	3 (10)
Change in medication between 1st and 2nd CTMPI	4 (13)

Except where indicated, data are numbers of patients (percentages). PCI=Percutaneous coronary intervention; CABG=Coronary artery bypass grafting; ACE/ARB=Angiotensin-converting enzyme inhibitors / Angiotensin II receptor blockers; CTMPI=Computed tomography myocardial perfusion imaging; GLP-1 = Glucagon-like peptide-1; DPP-4 = Dipeptidyl peptidase-4.

Echocardiography revealed a mean left ventricular ejection fraction of 68 ± 7 % and wall motion abnormalities in 30 % of patients. The majority were on antiplatelet drugs (93 %) at the time of the first CTMPI, with other medications including calcium channel blockers (53 %) and ACE/ARB (57 %). There was a change in medication for 13 % of patients between the first and second CTMPI.

3.2. Imaging results

Table2 provided detailed imaging results. According to the CAD-RADS classification by CCTA, CAD-RADS 1 accounted for 20 % (6/30), CAD-RADS 2 for 13 % (4/30), CAD-RADS 3 for 43 % (13/30), CAD-RADS 4A for 7 % (2/30), CAD-RADS 4B for none, and CAD-RADS 5 for 10 % (3/30). The CCTA findings remained consistent across the two examinations, revealing no new cases of coronary stenosis in the 2nd CCTA images. Dynamic CTMPI results presented that the 1st and 2nd global MBFs were 139 ± 37 and 138 ± 39 mL/100 mL/min, respectively, and the 1st and 2nd remote MBFs were 163 ± 43 and 162 ± 45 mL/100 mL/min, respectively.

The dose-length product (DLP), measured in mGy*cm, was recorded for both CCTA and dynamic CTMPI: for the 1st and 2nd CCTA, the DLPs were 161 ± 89 and 153 ± 100, respectively; for the 1st and 2nd dynamic CTMPI, they were 243 ± 66 and 222 ± 54, respectively. The increase in heart rate during stress compared to rest was 14 ± 8 bpm for the 1st dynamic CTMPI and 15 ± 5 bpm for the 2nd dynamic CTMPI.

Table 2
Imaging results.

Characteristic	All patients (n = 30)
CAD-RADS (CCTA)	
1	6 (20)
2	4 (13)
3	13 (43)
4A	2 (7)
4B	0 (0)
5	3 (10)
Dynamic CTMPI (mL/100 mL/min)	
1st global MBF (mean ± SD)	139 ± 37
2nd global MBF (mean ± SD)	138 ± 39
1st remote MBF (mean ± SD)	163 ± 43
2nd remote MBF (mean ± SD)	162 ± 45

Except where indicated, data are numbers of patients (percentages). CAD-RADS=Coronary Artery Disease Reporting and Data System; CCTA=coronary computed tomography angiography; CTMPI=computed tomography myocardial perfusion imaging; MBF=myocardial blood flow.

3.3. Test-retest reproducibility of MBF obtained using dynamic CTMPI

There was an excellent linear correlation between 1st and 2nd global MBFs (r = 0.89 [95 % CI: 0.77–0.95]; p < 0.0001; Fig. 2-A), between 1st and 2nd remote MBFs (r = 0.88 [95 % CI: 0.75–0.94]; p < 0.0001; Fig. 2-B) and between 1st and 2nd MBFs in all segments (r = 0.82 [95 % CI: 0.80–0.84]; p < 0.0001; Fig. 2-C). Representative cases where distributions of MBF were similar between two cardiac tests were presented in Fig. 3.

ICC was 0.94 (95 % CI: 0.87–0.97), 0.93 (95 % CI: 0.86–0.97), and 0.90 (95 % CI: 0.89–0.91) between global 1st and 2nd global MBFs, between 1st and 2nd remote MBFs, and between 1st and 2nd MBFs in all segments.

Bland-Altman plots showed a mean difference of –0.7 mL/100 mL/min (95 % limits of agreement [LoA], –35.3 to 36.7 mL/100 mL/min) between 1st and 2nd global MBFs (Fig. 4-A), of –1.3 mL/100 mL/min (95 % LoA, –42.4 to 45.0 mL/100 mL/min) between 1st and 2nd remote MBFs (Fig. 4-B) and of 0.7 mL/100 mL/min (95 % LoA, –48.6 to 50.0 mL/100 mL/min) between 1st and 2nd MBFs in all segments (Fig. 4-C).

3.4. Visual evaluation of the ability to detect abnormal perfusion on the dynamic CTMPI map

Inter-test agreement for visually detecting and grading abnormal perfusion suggesting ischemia on the CTMPI map was good with a weighted kappa value of 0.80 (95 % CI: 0.75–0.85) as shown in Fig. 5. In 289 segments with Grade 0 on the 1st CTMPI map, 249 segments (86 %) were found to be Grade 0, 28 (10 %) Grade 1, 11 (4 %) Grade 2, and 1 (0.3 %) Grade 3 on the 2nd CTMPI map. In 101 segments with Grade 1 on the 1st CTMPI map, 15 segments (15 %) were found to be Grade 0, 65 (65 %) Grade 1, 18 (18 %) Grade 2, and 3 (3 %) Grade 3 on the 2nd CTMPI map. In 62 segments with Grade 2 on the 1st CTMPI map, 3 segments (5 %) were found to be Grade 0, 16 (26 %) Grade 1, 38 (61 %) Grade 2, and 5 (8 %) Grade 3 on the 2nd CTMPI map. In 28 segments with Grade 3 on the 1st CTMPI map, 6 segments (21 %) were found to be Grade 2, and 22 (79 %) Grade 3 on the 2nd CTMPI map while no segments were rated as Grade 0 and Grade 1.

4. Discussion

To the best of our knowledge, this is the first study to examine the reproducibility of MBF values quantified with dynamic CTMPI. The main results were that dynamic CTMPI had the ability to reproduce absolute MBF values across multiple tests on the same patient and the consistency in the presence and severity of abnormal perfusion that suggests ischemia between the tests.

CAD and CMD are two distinct but related conditions affecting the heart's blood vessels. CAD involves the buildup of plaque in the epicardial coronary arteries. This buildup narrows the arteries, reducing blood flow and potentially leading to chest pain (angina), heart attacks, or heart failure [11]. On the other hand, CMD affects the heart's smaller blood vessels and is characterized by impaired blood flow due to damage to the inner walls of those vessels, leading to spasms and decreased blood flow to the heart muscle without the presence of significant plaque buildup seen in CAD [12]. CMD can cause symptoms similar to CAD, such as chest pain and shortness of breath, but is diagnosed and managed differently, requiring specialized tests to detect. Diagnosing CMD can be challenging due to the small size of the vessels involved, which are not easily visualized with standard imaging techniques as performed for CAD assessment. Although invasive angiography plays a crucial role in diagnosing CMD, invasive tests such as intracoronary Doppler wire and thermodilution are used to measure blood flow and resistance within the coronary microcirculation [13]. These tests can evaluate parameters like coronary flow reserve (CFR) and index of microcirculatory resistance (IMR), which provide information about the functional status of the smaller vessels. A reduced CFR or an elevated IMR indicates impaired microvascular function, suggesting CMD.

PET imaging is a highly effective non-invasive tool for assessing myocardial perfusion and the functional status of the heart's microvasculature. The high diagnostic performance of stress H_2O-PET MPI for

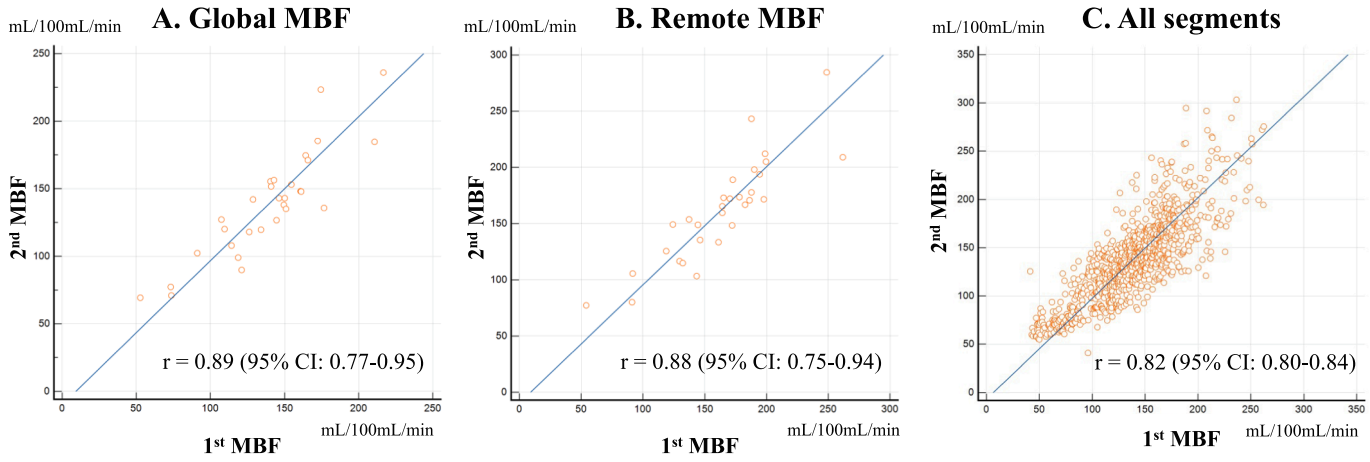

Fig. 2. Correlation between 1st and 2nd MBF obtained by dynamic CTMPI. There was an excellent linear correlation (A) between 1st and 2nd global MBFs (r = 0.89 [95 % CI: 0.77–0.95]; p < 0.0001), (B) between 1st and 2nd remote MBFs (r = 0.88 [95 % CI: 0.75–0.94]; p < 0.0001), and (C) between 1st and 2nd MBFs in all segments (r = 0.82 [95 % CI: 0.80–0.84]; p < 0.0001). CTMPI=computed tomography myocardial perfusion imaging; MBF=myocardial blood flow.

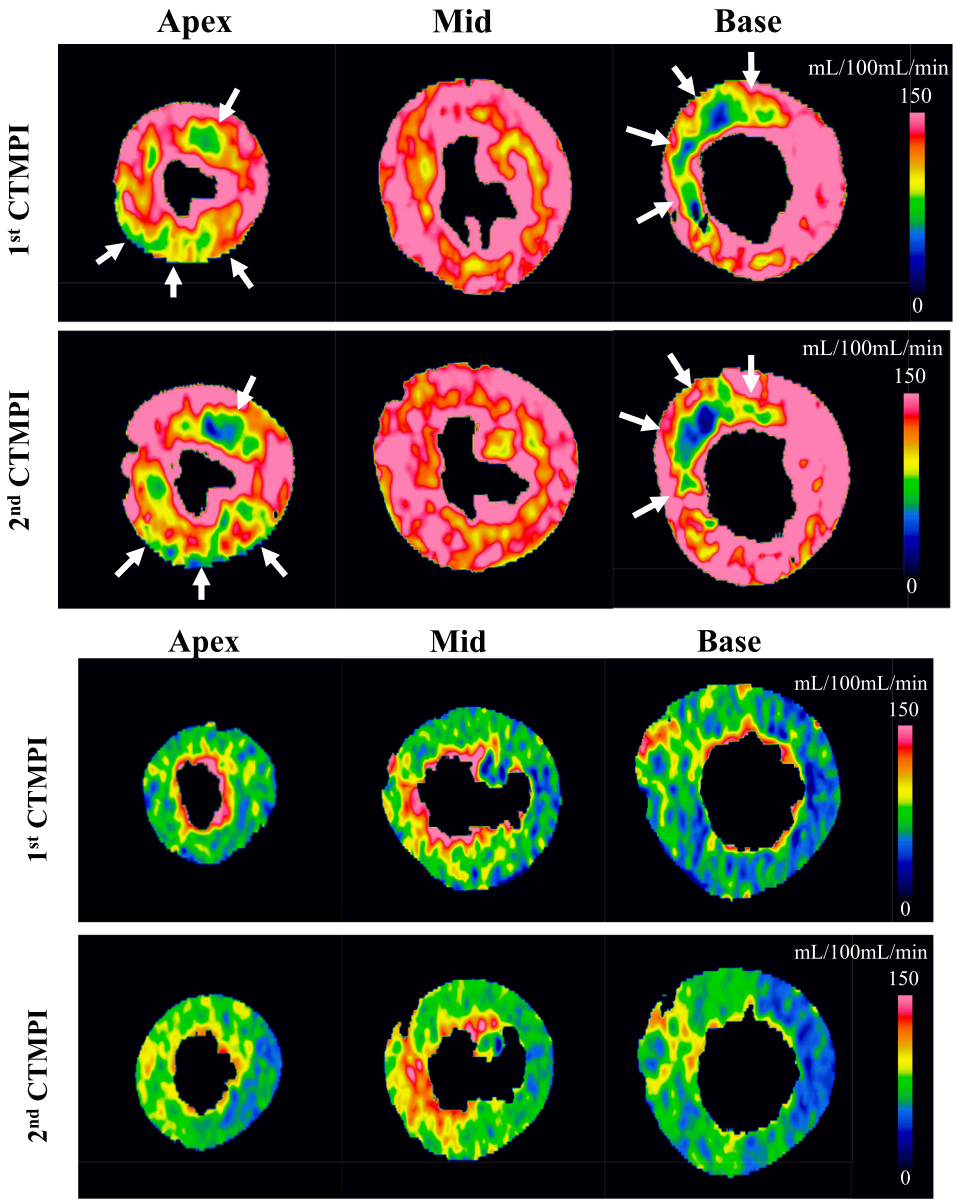

Fig. 3. Representative cases that show the test–retest reproducibility of MBF obtained by dynamic CTMPI. (A) Images in a 77 year-old-woman with chest pain and diabetes. The figures showed short-axis images on MBF maps obtained by 1st (upper section) and 2nd (lower section) dynamic CTMPI. In both the 1st and 2nd MBF maps, severe reductions in MBF (arrows) were similarly observed in the anterior and inferior walls of the apex and in the anteroseptal wall of the base. In the mid, mild reductions in MBF were detected circumferentially in the subendocardial pattern, consistent between the 1st and 2nd MBF maps. (B) Images in a 68 year-old-man with chest pain, diabetes and hyperlipidemia. The figures showed short-axis images on MBF maps obtained by 1st (upper section) and 2nd (lower section) dynamic CTMPI. The CTMPI maps from both examinations revealed circumferential reduced MBF, particularly in the lateral wall, extending from the base to the apex. CTMPI=computed tomography myocardial perfusion imaging; MBF=myocardial blood flow.

CAD has been well-documented, with studies using hyperemic MBF derived from stress H_2O-PET MPI revealing a diagnostic accuracy of 92 % for detecting CAD using fractional flow reserve as the reference [14] and superior diagnostic accuracy compared to CCTA and single photon emission computed tomography [15]. Additionally, the test–retest reproducibility of MBF and CFR estimates is reported to be very good, with a correlation coefficient (R2) of 0.935 for MBF in repeated Rb-PET studies, indicating PET's reliability and repeatability [16]. The same study showed that the low intra- and interobserver variability further confirms the robustness of MBF quantitation against different observers' analyses. This consistency across repeated studies is critical for the clinical utility of PET in diagnosing CAD and CMD. Furthermore, reduced MBF and CFR identified by PET imaging was associated with a higher risk of major adverse cardiovascular events [17], emphasizing the utility of stress PET MPI in identifying CMD that presents as reductions in hyperemic MBF and CFR.

Dynamic CTMPI presents an alternative non-invasive method for assessing MBF, with high diagnostic accuracy for detecting myocardial ischemia [8]. Dynamic CTMPI offers several advantages over MRI MPI and nuclear MPI. One key benefit is that it can be performed concurrently with CCTA, enabling comprehensive assessment of CAD by evaluating both anatomical stenosis and functional perfusion within a single session. A recent multi-center study [9] demonstrated that combining dynamic CTMPI with CCTA significantly improved diagnostic performance, increasing the area under the curve from 0.65 to 0.74 for identifying hemodynamically significant stenosis. In addition, given that CCTA has a high negative predictive value for excluding CAD, reduced MBF in patients without significant coronary stenosis on CCTA

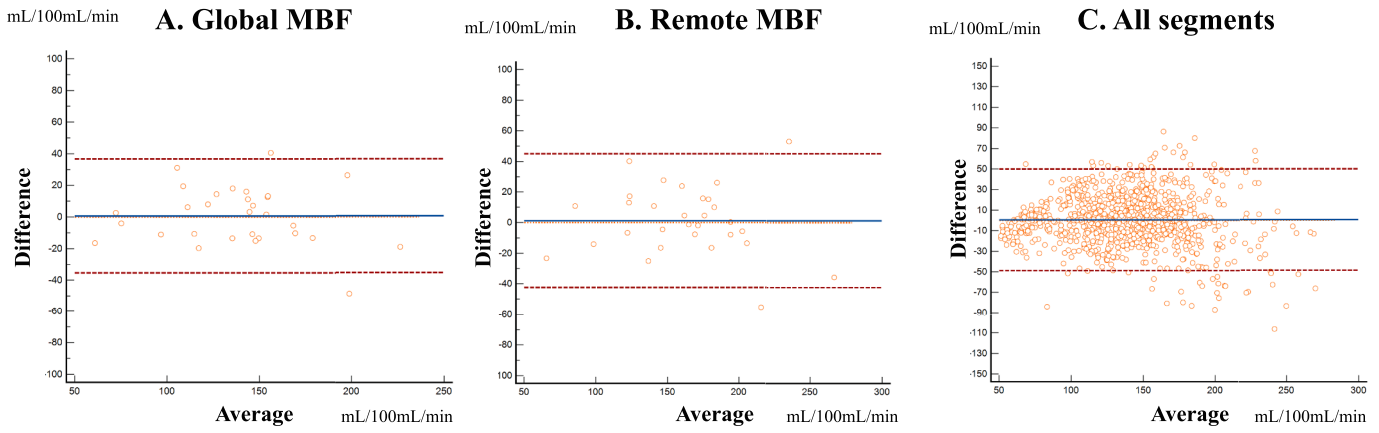

Fig. 4. Bland-Altman plots from 1st and 2nd MBF obtained by dynamic CTMPI. Bland-Altman plots showed a mean difference of –0.7 mL/100 mL/min (95 % limits of agreement [LoA], –35.3 to 36.7 mL/100 mL/min) between 1st and 2nd global MBFs (A), of –1.3 mL/100 mL/min (95 % LoA, –42.4 to 45.0 mL/100 mL/min) between 1st and 2nd remote MBFs (B) and of 0.7 mL/100 mL/min (95 % LoA, –48.6 to 50.0 mL/100 mL/min) between 1st and 2nd MBFs in all segments (C). CTMPI=computed tomography myocardial perfusion imaging; MBF=myocardial blood flow.

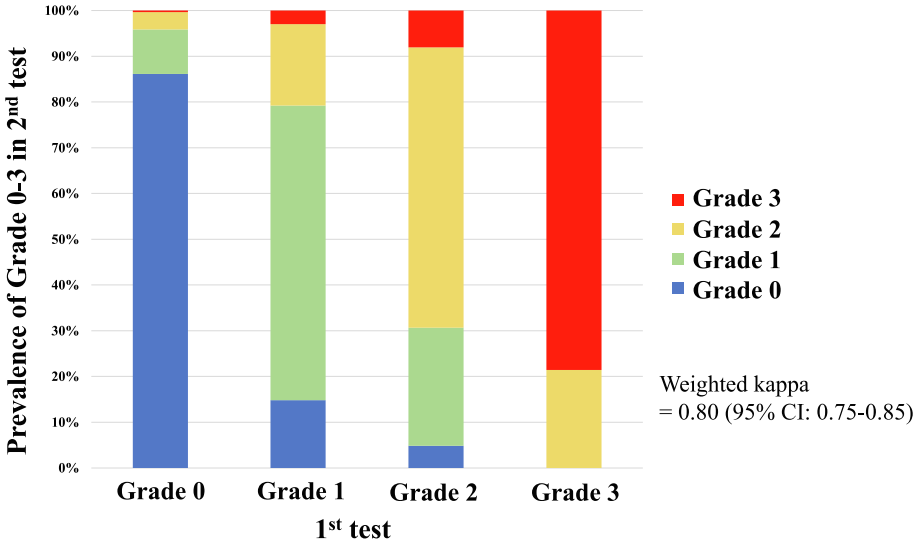

Fig. 5. Inter-test agreement for visual assessment of abnormal perfusion. Inter-test agreement for detecting abnormal perfusion visually on the CTMPI map was good with a weighted kappa value of 0.80 (95 % CI: 0.75–0.85). In 289 segments with Grade 0 on the 1st CTMPI map, 249 segments (86 %) were found to be Grade 0, 28 (10 %) Grade 1, 11 (4 %) Grade 2, and 1 (0.3 %) Grade 3 on the 2nd CTMPT map. In 101 segments with Grade 1 on the 1st CTMPI map, 15 segments (15 %) were found to be Grade 0, 65 (65 %) Grade 1, 18 (18 %) Grade 2, and 3 (3 %) Grade 3 on the 2nd CTMPT map. In 62 segments with Grade 2 on the 1st CTMPI map, 3 segments (5 %) were found to be Grade 0, 16 (26 %) Grade 1, 38 (61 %) Grade 2, and 5 (8 %) Grade 3 on the 2nd CTMPT map. In 28 segments with Grade 3 on the 1st CTMPI map, 6 segments (21 %) were found to be Grade 2, and 22 (79 %) Grade 3 on the 2nd CTMPT map while no segments were rated as Grade 0 and Grade 1. CTMPI=computed tomography myocardial perfusion imaging; MBF=myocardial blood flow.

may suggest the presence of CMD. In this respect, the advantage of combining CCTA with CTMPI is twofold: the combination allows for the simultaneous evaluation of obstructive CAD and myocardial ischemia and facilitates the diagnosis of CMD after CAD has been excluded. Another advantage of CTMPI is its shorter acquisition time compared to other modalities, offering greater convenience for patients and the potential for improved throughput in clinical practice [18]. CTMPI also allows for high-resolution imaging, which aids in detecting small-scale blood flow abnormality [19].

Despite these advantages of dynamic CTMPI, the test–retest reproducibility of MBF measurements obtained using dynamic CTMPI remains uninvestigated. The current study demonstrated that dynamic CTMPI can reproduce absolute MBF values across multiple tests on the same patient and revealed consistency in the detection and severity of abnormal perfusion that suggests ischemia between the tests. This reproducibility is crucial for ensuring that reduction in MBF measurements reflect true physiological changes rather than variability in the imaging technique itself. The results of our study were consistent with those of studies using stress PET MPI that investigated the test–retest reproducibility [16]. By reliably measuring MBF, dynamic CTMPI can help in determining the presence, extent, and severity of CAD and CMD, providing valuable information that can guide clinical decision-making. This is particularly important for CMD, which often goes undetected by traditional imaging methods focused on the epicardial coronary arteries. On the other hand, the consistent detection of abnormal perfusion suggestive of ischemia across tests further emphasize the potential of dynamic CTMPI as a robust tool for the evaluation of CAD. The robustness of dynamic CTMPI in reproducing MBF and consistently assessing ischemia may be useful not only in diagnosing CAD and CMD, but also in monitoring their progression and evaluating the effectiveness of therapeutic interventions. By offering a non-invasive means to quantify changes in MBF over time, it enables

clinicians to track the disease course and adjust treatment strategies accordingly. Nevertheless, further research is necessary to investigate the prognostic impact of CMD when diagnosed using dynamic CT MPI. Establishing the prognostic value of MBF obtained through this modality in relation to CMD will be essential for integrating dynamic CTMPI into routine clinical practice for the management of CMD.

The study has several limitations. Firstly, one of them is the study's retrospective, single-center design, which may limit the generalizability of the results to other settings. Future prospective, multicenter studies are needed to validate our findings and ensure broader applicability. Secondly, dynamic CTMPI requires the acquisition of multiple images over time to capture the passage of contrast through the myocardium, leading to higher radiation doses compared to single-phase imaging. While technological advancements have reduced these radiation doses [20], radiation exposure remains a concern. Thirdly, maximal upslope analysis of dynamic CTMPI employed in this study underestimated MBF when compared directly with H_2O-PET measurements. However, a prior study showed that this discrepancy was reduced by using a fitting equation to correct the MBF derived from dynamic CTMPI and that the corrected MBF values from dynamic CTMPI showed improved agreement with the MBF values from H_2O-PET [21]. Fourthly, another limitation of our study includes not only the inconsistency in the intervals between the test and retest but also the fact that these intervals were longer compared to previous studies [16,22]. Although the CCTA findings remained consistent across the two tests, those varied and extended time gaps might influence the physiological state of the patients, potentially affecting the comparability of the test results. To assess test–retest reproducibility more accurately, future studies should standardize the interval between examinations. Fifthly, the study population was relatively small, and patients without obstructive CAD on CCTA accounted for 33 % of the study population. Larger future studies that do not include patients with obstructive CAD may be required to assess the utility of CTMPI in the evaluation of CMD. Sixthly, although no patients had coronary revascularization between 1st CTMPI and 2nd CTMPI, 87 % of the patients had a history of coronary revascularization, which might have had affected MBFs in vascular territories influenced by stents or bypass grafts. Additionally, given the high prevalence of comorbidities and the variety of medications in the study population, these factors may have influenced the test–retest results. Seventhly, the study included only 25 % of the initial cohort, which may limit the generalizability of the results. Eighthly, our study did not include a comparator to established methods for evaluating myocardial perfusion, such as MRI, PET, or invasive assessments of fractional flow reserve and microcirculation indexes. Finally, the study did not include the assessment of CFR from dynamic CTMPI. A major challenge in measuring CFR with dynamic CTMPI is the necessity for two CT scans—one at rest and another during stress. This requirement increases the patient's exposure to radiation and the amount of contrast agent used.

5. Conclusion

Dynamic CTMPI can consistently reproduce absolute MBF values and reliably detect myocardial perfusion abnormalities. When complemented by the anatomical insights for CAD provided by CCTA, dynamic CTMPI may become a robust, non-invasive diagnostic tool that enables the evaluation of the presence and severity of myocardial ischemia and CMD.

6. Disclosure

Department of Advanced Diagnostic Imaging where Drs. Nakamura and Kitagawa currently belong to is an endowment department supported with an unrestricted grant from Siemens Japan. All other authors have reported that they have no relationships relevant to the contents of this paper to disclose.

CRediT authorship contribution statement

Daisuke Hasegawa: Writing – original draft, Resources. **Satoshi Nakamura:** Writing – review & editing, Methodology, Data curation. **Masafumi Takafuji:** Writing – review & editing. **Hajime Sakuma:** Supervision. **Kakuya Kitagawa:** Writing – review & editing, Conceptualization.

Declaration of competing interest

The authors declare that they have no known competing financial interests or personal relationships that could have appeared to influence the work reported in this paper.

References

[1] J.A. Panza, Myocardial ischemia and the pains of the heart, N. Engl. J. Med. 346 (25) (2002) 1934–1935.
[2] P. Theroux, V. Fuste, Acute coronary syndromes: unstable angina and non–Q-wave myocardial infarction, Circulation 97 (12) (1998) 1195–1206.
[3] A. Abbate, G.G. Biondi-Zoccai, P. Agostoni, et al., Recurrent angina after coronary revascularization: a clinical challenge, Eur. Heart J. 28 (9) (2007) 1057–1065.
[4] F. Spione, V. Arevalos, R. Gabani, et al., Coronary microvascular angina: a state-of-the-art review, Front. Cardiovasc. Med. 9 (2002) 800918.
[5] H. Aldiwani, S. Mahdai, G. Alhatemi, et al., Microvascular angina: Diagnosis and management, Eur. Cardiol. Rev. 16 (2021).
[6] J.M. Lee, J. Layland, J.H. Jung, et al., Integrated physiologic assessment of ischemic heart disease in real-world practice using index of microcirculatory resistance and fractional flow reserve: insights from the International Index of Microcirculatory Resistance Registry, Circ. Cardiovasc. Interv. 8 (11) (2015) e002857.
[7] R.S. Driessen, P.G. Raijmakers, W.J. Stuijfzand, et al., Myocardial perfusion imaging with PET, Int. J. Cardiovasc. Imaging 33 (2017) 1021–1031.
[8] K. Kitagawa, Y. Goto, S. Nakamura, et al., Dynamic CT perfusion imaging: state of the art, Cardiovasc. Imag. Asia 2 (2) (2018) 38–48.
[9] K. Kitagawa, S. Nakamura, H. Ota, et al., Diagnostic performance of dynamic myocardial perfusion imaging using dual-source computed tomography, J. Am. Coll. Cardiol. 78 (20) (2021) 1937–1949.
[10] F.M. Nous, T. Geisler, M.B. Kruk, et al., Dynamic myocardial perfusion CT for the detection of hemodynamically significant coronary artery disease, J. Am. Coll. Cardiol. Img. 15 (1) (2022) 75–87.
[11] E.G. Nabel, E.A. Braunwald, Tale of coronary artery disease and myocardial infarction, N. Engl. J. Med. 366 (1) (2012) 54–63.
[12] P.G. Camici, F. Crea, Coronary microvascular dysfunction, N. Engl. J. Med. 356 (8) (2007) 830–840.
[13] R. Rehan, A. Yong, M. Ng, et al., Coronary microvascular dysfunction: a review of recent progress and clinical implications, Front. Cardiovasc. Med. 10 (2023) 1111721.
[14] S. Kajander, E. Joutsiniemi, M. Saraste, et al., Cardiac positron emission tomography/computed tomography imaging accurately detects anatomically and functionally significant coronary artery disease, Circulation 122 (6) (2010) 603–613.
[15] I. Danad, P.G. Raijmakers, R.S. Driessen, et al., Comparison of coronary CT angiography, SPECT, PET, and hybrid imaging for diagnosis of ischemic heart disease determined by fractional flow reserve, JAMA Cardiol. 2 (10) (2017) 1100–1107.
[16] G. El Fakhri, A. Kardan, A. Sitek, et al., Reproducibility and accuracy of quantitative myocardial blood flow assessment with 82Rb PET: comparison with 13N-ammonia PET, J. Nucl. Med. 50 (7) (2009) 1062–1071.
[17] B.A. Herzog, L. Husmann, I. Valenta, et al., Long-term prognostic value of 13N-ammonia myocardial perfusion positron emission tomography: added value of coronary flow reserve, J. Am. Coll. Cardiol. 54 (2) (2009) 150–156.
[18] O. Sliwicka, I. Sechopoulos, A. Baggiano, et al., Dynamic myocardial CT perfusion imaging—state of the art, Eur. Radiol. 33 (8) (2023) 5509–5525.
[19] E. Tonet, G. Pompei, E. Faragasso, et al., Coronary microvascular dysfunction: PET, CMR and CT assessment, J. Clin. Med. 10 (9) (2021) 1848.
[20] M. Fujita, K. Kitagawa, T. Ito, et al., Dose reduction in dynamic CT stress myocardial perfusion imaging: comparison of 80-kV/370-mAs and 100-kV/300-mAs protocols, Eur. Radiol. 24 (2014) 748–755.
[21] M. Takafuji, K. Kitagawa, M. Ishida, et al., Clinical validation of the accuracy of absolute myocardial blood flow quantification with dual-source CT using 15O-Water PET, Radiol. Cardiothorac. Imag. 3 (5) (2021) e210060.
[22] C. Byrne, A. Kjaer, N.E. Olsen, et al., Test–retest repeatability and software reproducibility of myocardial flow measurements using rest/adenosine stress Rubidium-82 PET/CT with and without motion correction in healthy young volunteers, J. Nucl. Cardiol. 28 (2021) 2860–2871.